EFFECT OF La^{+3} IONS ON NICKEL -CADMIUM SPINEL FERRITES SYNTHESIZED BY Co-PRECIPITATION METHOD

M. I. ARSHAD[a], S. IKRAM[a], K. MAHMOOD[a], A. ALI[a], A. UN NABI[a], N. AMIN[a], Y. AROOJ[b] , N. SAWAIRA[b], M. ASGHAR[c], M. SALEEM[d], F. JABEEN[e], J. BATOOL[b], G. MUSTAFA[f*]

[a]*Department of Physics, G.C. University Faisalabad 38000, Pakistan*
[b]*Department of Physics GCW University Faisalabad 38000, Pakistan*
[c]*Department of Physics, the Islamia University of Bahawalpur, Pakistan.*
[d]*Departments of Physics, LUMS University Lahore, Pakistan*
[e]*CCAST, North Dakota State University, Fargo, ND, United States*
[f]*Department of Physics, Bahauddin Zakariya University Multan 60800, Pakistan*

The effect of rare earth metal La^{3+} ions on structural, optical and electrical properties of $Ni_{0.3}Cd_{0.7}La_xFe_{2-x}O_4$, (x=0, 0.01, 0.02, 0.03, 0.04, & 0.05) ferrites were investigated. The co-precipitation method was used for the preparation of these nano-crystalline and characterized by XRD, EDX, SEM, FTIR, UV Vis and I-V techniques. An XRD pattern of the entire sample reveals the formation spinel cubic structure of the ferrites powder. The crystallite size was measured and was found to be in the range from (21 nm -29nm). SEM images revealed with doping of La^{3+} content and grain size was found to be increased. The optical properties were investigated from UV/Vis technique and shows that absorption decreases with increases of lanthanum content. The two strong absorption bands were observed 442 cm^{-1} and 532.44 cm^{-1} from FTIR and gives good agreement with spinel ferrites. The electrical resistivity of materials was found to be varies in the range (4.5×10 -1.9×10^{-8} ohm-cm) with doping of La^{3+} ion investigated from I-V tow probe method. Hence, the observed result exposed that the structural, optical and electrical properties have strongly effected with doping of lanthanum content.

(Received October 19, 2017; Accepted January 8, 2018)

Keywords: Spinel ferrites, co-precipitation; XRD, UV/vis; I-V (Resistivity)

1. Introduction

Ferrites become an interesting group of magnetic materials owing to their unique and versatile properties such as mechanical hardness, low inherent toxicity, high electrical resistivity, low electric loss, physical and chemical stabilities, magneto optical properties and saturation magnetization [1, 2]. Ferrites have wide range of applications in many fields such as gas sensing transformer cores, electromagnetic interference (EMI), magnetic amplifiers, antenna rods, catalysis multilayer chip inductor, power transformer in electronic circuits, magnetic resonance imaging and in biomedicine etc. Due to this wide range of applications, these materials have been much attention for all researchers in the world [3-5]. Ferrites found to be good magnetic materials and with the choice of cations scattering concerning the octahedral and tetrahedral positions of spinel lattice, their properties can be changed. The synthesis techniques, doping element, sintering heat and element compositions have also influenced on their properties [6]. Spinel ferrites are class of thermally and chemically stable materials with general formula AB_2O_4 . With the trivalent ion being iron, theses ferrites have spinel structure. Due to structural, electrical and catalytic properties, these spinel ferrites have received much fundamental and technological importance [7]. The various preparation techniques such as sol-gel, micro-emulsion, polymer pyrolysis, combustion and hydrothermal method can be utilized for the synthesis of spinel ferrites. The Co-precipitation method found to be a attractive preparation technique than others because of their

*Corresponding author: ghulammustafabzu@gmail.com

several advantages such as high homogeneity, particle size etc.[8]. Many researchers have studied the Cd-substituted ferrite with other metal ions such as (Ni, Mg, Mn, Zn, Cd and Co) and found it an important member of a spinel class of ferrimagnetic materials. The ferrites have low dielectric loss, high resistivity, high Curie temperature, low cost, high soaking magnetization and became an attractive material for microwave applications. It has been reported that various properties of ferrites can originate from their ability to incorporate a variety of rare earth metal ions or transition metal ions into their lattice which causes change in structural, magnetic and optical and electrical properties. These changes are due to reordering of the cations among octahedral and tetrahedral sites of the ferrite lattice. Ashok and Shelar et al [9, 10] also reported the same composition with different method of preparation as well as sintering conditions. Rezlesecu et al [11] reported that the addition of rare earth metal ion in ferrites changes their structural and electrical properties. In the present study, the Ni-Cd spinel ferrites with La ions are chosen to investigate the structural, optical and electrical properties.

2. Material and method

2.1 Sample Preparation

The spinel ferrites having general formula $Ni_{0.3}Cd_{0.7}$ $La_xFe_{2-x}O_4$ (x = 0, 0.01, 0.02, 0.03, 0.04, & 0.05) was prepared by using co-precipitation technique with stoichiometric proportions of material $Ni(NO_3)_2.6H_2O$, $CdCl_2$ .6 H_2 O, $FeCl_3$ and $La(NO_3)_3$.$6H_2$ O. The desired quantities of all chemicals are dissolved in deionized water separately. After thoroughly mixing of all solutions on hot plate of magnetic stirrer at 60 ^oC, NaOH was added dropwise in mixture to maintain pH 11. The precipitates of the solutions were formed and placed in the preheated water bath at 90 ^oC for 2 h. Then these precipitates were washed with deionized water twice a time and then dried in oven at 85 ^oC for 24 h. Finally, the dried powder and pellet of all the samples was sintered at 850 ^oC for 2 h.

3. Characterization of the materials

The structural properties and phase identification was measured by XRD using Philip Analytical diffract meter operating at 30 mA and 40 KV. The scanning electron microscope (SEM) armed with energy-dispersive X-ray (EDX) confirmed the apparent morphology and elemental composition. UV/Vis and I-V tow probe techniques are used for electrical analysis.

3.1 Microstructural Study

Fig 1 shows the XRD patterns of $Ni_{0.3}Cd_{0.7}La_xFe_{2-x}O_4$ (x = 0, 0.01, 0.02, 0.03, 0.04 & 0.05) ferrites synthesized by co-precipitation methods. A single phase structure along with few trace of secondary phases was observed. The observed patterns have prominent diffraction peaks with these reflection planes (220), (311), (400), (422) and (511) which is indexed by computer software. The XRD patterns also reflected iron oxide (β-phase) [12]. The secondary phase at grain boundary for $LaFeO_3$ is attributed by peak corresponding to (2θ =32.27). It was observed that as well as La^{3+} content is increase in leads to improvement in the intensity of orthoferrite. Another secondary phase peaks identified at (2θ = 33.14) named as Fe_2O_3 (COD 9015964) [13]. The solubility limited of La^{3+} ion with iron oxide into the spinel lattice main cause to secondary phases appeared on the grain boundaries [14]. The lattice constant “a” and volume of unit cell “V” was analyzed by following equation:

$$A = d\sqrt{h2 + k2 + l2} \quad (1)$$

$$V = a^3 \quad (2)$$

Where (h, k, l) is called miller indices and d is inter-plane distance. For the sharpest peak (311) in XRD patterns, the crystalline size of the entire sample was measured by using Scherer Equation:

$$D = \frac{0.9\,\lambda}{\beta cos\theta} \tag{3}$$

Where β is the line broadening at FWHM in radians, θ is Bragg angle and X-ray wavelength is λ=1.542Å [15-17].

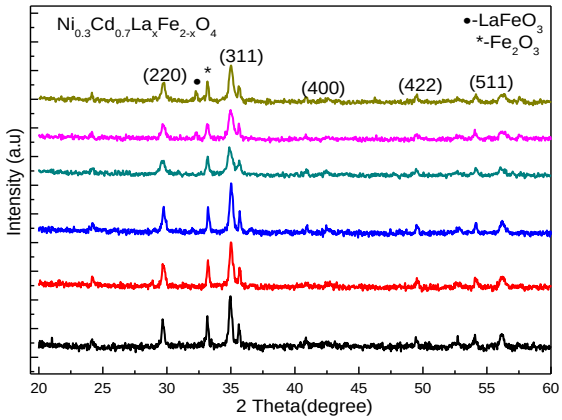

Fig. 1. XRD Patterns of $Ni_{0.3}Cd_{0.7}La_xFe_{2-x}O_4$ (x=0, 0.01, 0.02, 0.03, 0.04 & 0.05)

Table 1. Lattice constant, Crystallite size (nm), Absorption, Energy band gap (eV) and electrical resistivity (ohm-cm) of $Ni_{0.3}Cd_{0.7}La_xFe_{2-x}O_4$

Composition	Lattice Constant (Å)	Crystallite Size (nm)	Absorption (a.u)	Energy band gap (eV)	Electrical resistivity (ohm-cm)
$Ni_{0.3}Cd_{0.7}Fe_2O_4$	8.504	29.9	1.47	1.96	4.7×10^8
$Ni_{0.3}Cd_{0.7}La_{0.01}Fe_{1.99}O_4$	8.502	25.7	1.09	2.19	4.8×10^8
$Ni_{0.3}Cd_{0.7}La_{0.02}Fe_{1.98}O_4$	8.502	25	0.92	2.39	4.9×10^8
$Ni_{0.3}Cd_{0.7}La_{0.03}Fe_{1.97}O_4$	8.506	22.4	0.70	2.57	5.2×10^8
$Ni_{0.3}Cd_{0.7}La_{0.04}Fe_{1.96}O_4$	8.499	21.7	0.37	2.59	6.2×10^8
$Ni_{0.3}Cd_{0.7}La_{0.05}Fe_{1.95}O_4$	8.494	21.2	0.25	3.02	6.8×10^8

The physical parameters are measured from the XRD data and obtained values are listed in the Table 1. It was observed that the crystallite size was decreased by increasing of La^{+3} ion content. Similar trend in the crystallite size was found in the literature [18]. Due to large difference in ionic radii between Fe^{3+} (0.645Å) and La^{3+} (1.6061Å) ion, a minor change observed in the lattices constant. The lattice constant should be embellished with La^{3+} content due to replacement of Fe^{3+} with La^{3+} ion content attributed to solidity of spinel lattice via secondary parts [14, 19].

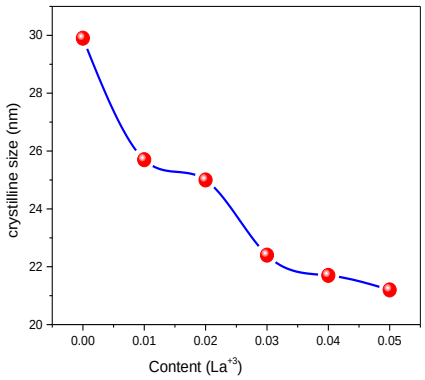

Fig. 2. Crystalline Size (nm) vs content (La^{+3})

3.2 Morphological Analysis

The SEM images of $Ni_{0.3}$ $Cd_{0.7}La_xFe_{2-x}O_4$ nanoparticles (x = 0.00, 0.01, 0.03 & 0.05) are shown in Fig 2. The observed that the distribution of the grain is uniformed and grain size was estimated by line intercept method. It was clearly seen that from images the grain size varied with the increasing of the lanthanum ion which proceeding disbursement of cation positions in lattice[20].

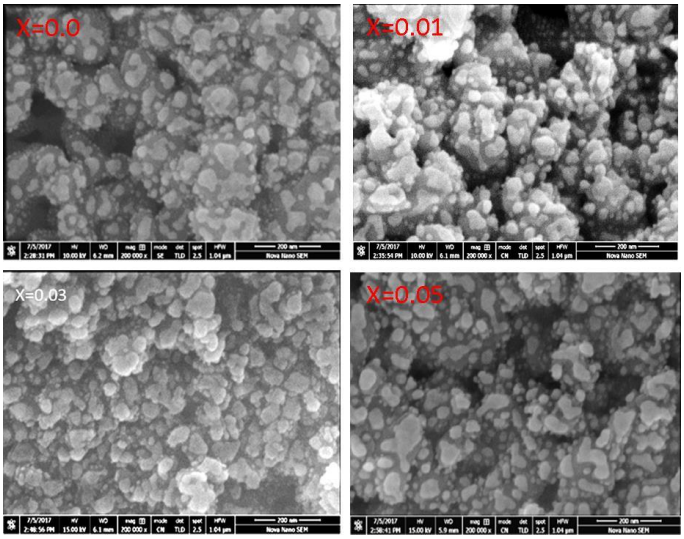

Fig. 2. Morphological analysis for $Cd_{0.7}Ni_{0.3}La_xFe_{2-x}O_4$ (x=0, 0.01, 0.03 & 0.05)

The fact is that SEM analysis gives extent of secondary particles self-possessed by several crystallites through easy reunification while XRD analysis gives only size of single crystallite[21].

3.3 Energy dispersive X-ray (EDX) Analysis

The energy dispersive X-ray analysis of descriptive sample was shown in Fig 3. The existence of elements Fe, Ni, Cd, La and O was confirmed by spectra. The obtained atomic percentage of each element used in the synthesized product was listed in the Table 2. It was observed from the Table 2., the element Cd is volatile at higher temperature and obtained atomic percentage is reduced at some extent.

Table 2: The elemental composition of $Ni_{0.3}Cd_{0.7}La_xFe_{2-x}O_4$

Elements	X=0.01	X= 0.03	X = 0.05
C Atomic (%)	14.82	27.03	14.5
O Atomic (%)	55.84	50.34	55.29
Fe Atomic (%)	24.24	19.25	23.28
Cd Atomic (%)	2.48	1.61	3.26
Ni Atomic (%)	2.53	1.64	2.87
La Atomic (%)	0.09	0.13	0.8

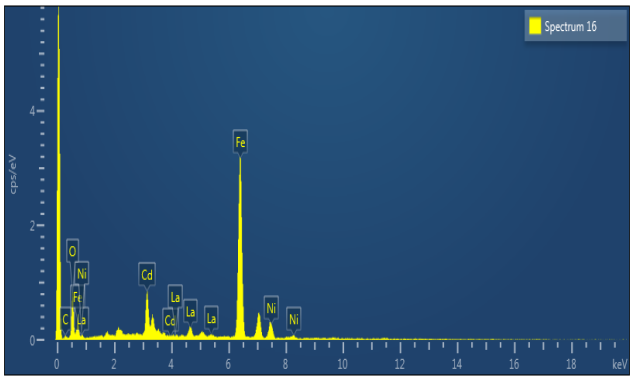

Fig. 3. EDX of $Ni_{0.3}Cd_{0.7}La_{0.01}Fe_{1.99}O_4$ ferrites

3.4 FTIR analysis

The FTIR bands of nanocrystalline **$Ni_{0.3}Cd_{0.7}$ $La_{0.01}Fe_{1.99}O_4$ ferrite was** recorded in the range 400-4000cm^{-1} as shown in Fig. 4. The two absorption band Octahedral (v_1) and tetrahedral (v_2) was observed respectively[22]. FTIR analysis gives absorption band around 532.44 cm^{-1} tetrahedral while 442 cm^{-1} octahedral sites. Through this analysis it was confirmed that the phase identification, (M-O) metal oxide group exist in the presented sample.

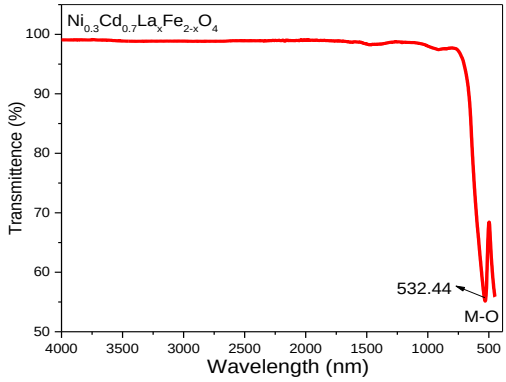

Fig. 4. FTIR spectrum of $Ni_{0.3}Cd_{0.7}La_{0.01}Fe_{1.99}O_4$ ferrites

3.5 Ultra-Violet Visible Spectroscopy Analysis

There are different ways for the optical analysis but one of the attractive techniques to study optical properties is ultra-violet visible spectroscopy. The solution of Ni-Cd ferrites was synthesized by utilizing deionized water as solvent. The UV/vis spectrum was shown in Fig. 6 which is recorded in the range of 1.5-4 eV. The absorption spectrum of Ni-Cd nanoferrites gives good absorption in the range of visible region 340-400 nm. The highest absorption was analyzed around the 380 nm and 1.47cm^{-1} respectively. The absorption wavelength has an inverse relation

with energy band gap and size of nanoparticles [23]. By employed following Tauc model relation, energy band gap can be calculated.

$$E=\frac{hc}{\lambda} \quad (4)$$

From absorption peaks, it was observed that absorption intensity decreasing with increasing La^{+3} content also reduce in particle size. Such kind of behavior found in the semiconductors materials which is reported in the literature [24]. A small peak shift was observed from 386nm to 384nm with maximum La^{+3} content which causes enhancement of energy band gap [25]. It is clearly shown that the role of the particle size effected on the optical properties. In Fig.6 shows the comparison between absorption and (T %) relation in the range 1.5 -4 eV and also determined the bandgap energy at n=0.5 .The obtained values is listed in the Table1.

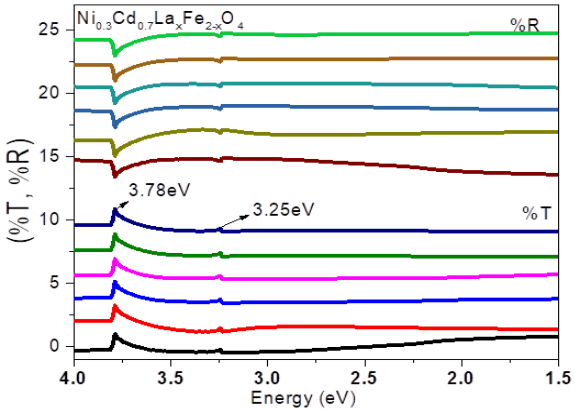

Fig. 6. UV Vis (%T,%A) transmittance and absorption spectrum for $Ni_{0.3}Cd_{0.7}La_xFe_{2-x}O_4$ (x = 0, 0.01, 0.02, 0.03, 0.04, 0.05) ferrites

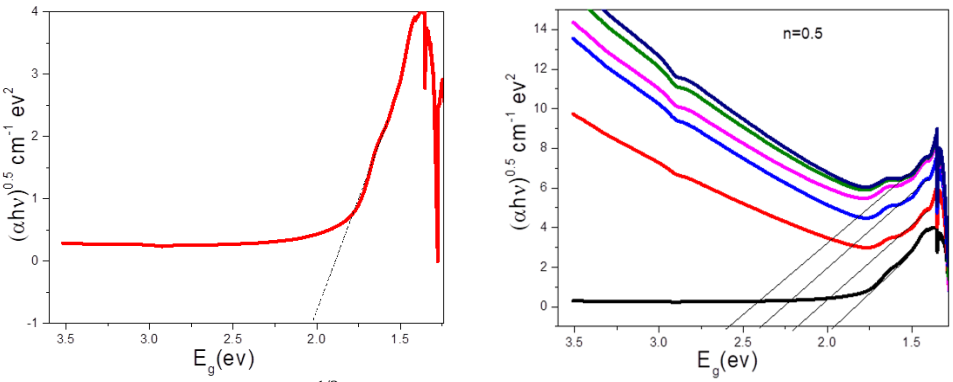

Fig. 7. Plot $(\alpha hv)^{1/2}$ versus $E_g(ev)$ of $Ni_{0.3}Cd_{0.7}La_xFe_{2-x}O_4$ ferrites

3.6. I-V Characterization

Fig 8 shows family of I-V curve for different samples at 550 ^oC temperature. The electric resistivity of all the samples measured by following relation [26]:

$$R=pL/A \quad (5)$$

Where A is the area, L is width and R is resistance of pellet.

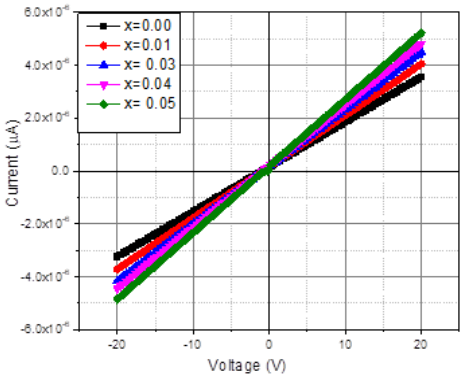

Fig. 8. I-V curves of $Ni_{0.3}Cd_{0.7}La_xFe_{2-x}O_4$ spinel ferrites at 550 ^oC

Table 1 shows value of electrical resistivity for all the samples with different La^{+3} content. The value of electrical resistivity was measured in the range of 4.7×10^8 to 6.8×10^8 (ohm-cm). The electrical resistivity has dependence on configuration of samples and crystal structure. The observed result exposed that electrical resistivity was increased with La^{+3} content, the similar resulted was reported by Kumar *et al;*[27] in his research work. In the UV/Vis analysis it was observed that band gap energy increase with La^{+3} content and it also causes of increasing in electrical resistivity. Fig 9 illustrates the effect of electrical resistivity with substitution of La^{+3} content.

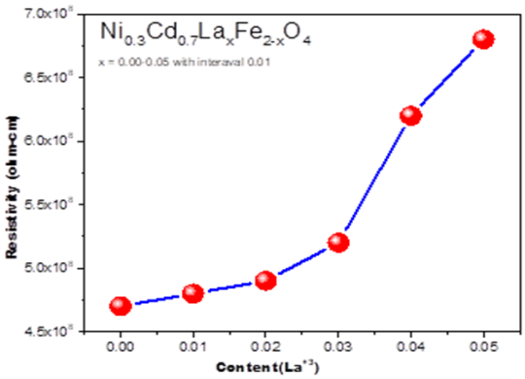

Fig. 9. Variation of electrical resistivity VS La^{+3} (content)

4. Conclusions

A series of $Ni_{0.3}Cd_{0.7}La_xFe_{2-x}O_4$ (x = 0, 0.01, 0.02, 0.03, 0.04 & 0.05) spinel ferrites synthesized by co-precipitation methods as confirmed by XRD analysis. The lattice constant lie in the range (8.494 Å - 8.504 Å) and the average crystallite size calculated using Scherrer's formula lie in the range of (21nm -29 nm). The optical band gap energy increased (1.96-3.02 eV) with increase of La^{+3}content due to the formation of oxygen vacancies and the induction of lattice distortions, SEM analysis confirmed the morphology of the synthesized material grain size growth decreased. The electrical resistivity was observed in the range 4.7×10^8 to 6.8×10^8 (ohm-cm).

Acknowledgements

The author (Ghulam Mustafa) is thankful to Higher Education Commission (HEC) of Pakistan for providing financial support to carry out this work under IRSIP scholarship.

References

[1] S. Ramesh, et al., Ceramics international **40**(6), 8729 (2014).
[2] T. Shinde, A. Gadkari, P. Vasambekar, Journal of Magnetism and Magnetic Materials **333,** 152 (2013).
[3] M. Rashad, et al., Journal of Alloys and Compounds, **486**(1), 759 (2009).
[4] Z. Chen, et al., Journal of Alloys and Compounds **609**, 21 (2014).
[5] S.-F. Wang, et al., Journal of Magnetism and Magnetic Materials, **365,** 119 (2014).
[6] I. Gul, A. Maqsood, Journal of Alloys and Compounds **465**(1), 227 (2008).
[7] N. Bahlawane, et al., Physical Chemistry Chemical Physics **11**(40), 9224 (2009).
[8] J. Xie, et al., Journal of magnetism and magnetic materials **314**(1), 37 (2007).
[9] A. Ashok, et al., World Journal of Condensed Matter Physics **2**(04), 257 (2012).
[10] M. Shelar, et al., Journal of Alloys and Compounds, **476**(1), 760 (2009).
[11] E. Rezlescu, et al., Crystal Research and Technology, **31**(3), 343 (1996).
[12] Y. Dasan, et al., PloS one, **12**(1), p. e0170075 (2017).
[13] C. Stergiou, G. Litsardakis. Structural and magnetic properties of yttrium and lanthanum-doped Ni-Co and Ni-Co-Zn spinel ferrites. in AIP Conference Proceedings. 2014. AIP.
[14] Y. Wang, et al., Journal of Magnetism and Magnetic Materials, **398**, 90 (2016).
[15] G. Mustafa, et al., Journal of Magnetism and Magnetic Materials **378,** 409 (2015).
[16] G. Mustafa, et al., Journal of Magnetism and Magnetic Materials **387,** 147 (2015).
[17] N. Amin, et al., Digest Journal of Nanomaterials and Biostructures, **11**(2), 579 (2016).
[18] S.M. Rathod, et al., Synthesis and Characterizationof La^{3+} Doped Ni NanoFerriteby Sol-Gel Method.
[19] N. Rezlescu, et al., Journal of Physics: Condensed Matter, **6**(29), 5707 (1994).
[20] A.I. Ali, et al., Journal of Materials Research and Technology **2**(4), 356 (2013).
[21] X.Wu, et al., Journal of Materials Science, **52**(17), 10085 (2017).
[22] A. Shitre, et al., Materials Letters, **56**(3), 188 (2002).
[23] M. Azim, et al., Digest Journal of Nanomaterials and Biostructures **11**(3), 953 (2016).
[24] S. Imran, et al., Digest Journal of Nanomaterials and Biostructures **11**(4), 1197 (2016).
[25] Y.-C.Ng, M. Shamsuddin, Journal of the Iranian Chemical Society **8,** S28 (2011).
[26] E. Barsoukov, J. R. Macdonald, Impedance spectroscopy: theory, experiment, and applications. 2005: John Wiley & Sons.
[27] P. Kumar, et al., Journal of Alloys and Compounds, **508**(1), 115 (2010).